Single molecule spectroscopy of polyfluorene chains reveals β-phase content and phase reversibility in organic solvents

Alfonso Brenlla[‡], Francisco Tenopala-Carmona[‡], Alexander L. Kanibolotsky[#,§], Peter J. Skabara[#*], Ifor D. W. Samuel[‡*], J. Carlos Penedo[‡,¶*]

[‡]Organic Semiconductor Centre, SUPA School of Physics and Astronomy, University of St Andrews, North Haugh, KY16 9SS, St Andrews, UK.

[#]WestCHEM, School of Chemistry, University of Glasgow, Joseph Black Building, University Avenue, Glasgow, G12 8QQ, UK.

[¶]School of Biology, Biomedical Science Research Complex, University of St Andrews, North Haugh, KY16 9ST, St Andrews, UK.

[§]Institute of Physical-Organic Chemistry and Coal Chemistry, 02160 Kyiv, Ukraine

Corresponding Author

jcp10@st-andrews.ac.uk; Peter.Skabara@glasgow.ac.uk; idws@st-andrews.ac.uk

Lead Contact

idws@st-andrews.ac.uk

KEYWORDS Conjugated polymers, surface-passivation, photoluminescence, β-phase structure, single-molecule detection

ABSTRACT: Conjugated polymers (CPs) are an important class of organic semiconductors that can be deposited from solution to make optoelectronic devices. Among them, poly(9,9'-dioctlyfluorene) (PFO) has distinctive optical properties arising from its ability to adopt an ordered planar conformation (b-phase) from a disordered glassy phase (a-phase). The b-phase has attractive optical properties, but the precise mechanism of its formation in solution remains unknown.

Here, we have combined specifically tailored polymer synthesis and surface-passivation strategies to provide the first spectroscopic characterization of single PFO chains in solution at room temperature. By anchoring PFO mole-

cules at one end on an anti-adherent surface, we show that isolated chains can adopt the b-phase conformation in a solvent-dependent manner. Furthermore, we find that individual PFO chains can reversibly switch multiple times between phases in response to solvent-exchange events. The methodology presented here for polymer synthesis and immobilization is widely applicable to investigate other luminescent polymers.

INTRODUCTION

Conjugated polymers (CPs) are π-delocalized light-emitting molecules widely used as active materials in optoelectronic devices, such as displays, solar cells and solid-state lasers.[1,2] Poly(dialkylfluorene)s constitute a particularly relevant class of conjugated polymers because of their emission in the deep-blue part of the spectrum and their high photoluminescence quantum yield and charge mobilities.[3] Poly(dialkylfluorene)s have also emerged as attractive materials to investigate the fundamental correlation between chain morphology and photophysical properties because of their intriguing ability to form different polymorphs depending on solution conditions.[4–6] It has been shown that spin-coating poly(9,9'-dioctlyfluorene) (PFO) from a good solvent results in films containing mostly disordered chains, commonly referred as α-phase (also known as glassy phase) (Figure S1a).[5–7] However, it was also shown that thermal cycling[5,8] and solvent swelling[8–10] could be used to induce a highly-organized structure with coplanar monomeric units and extended conjugation length, commonly referred to as the β-phase (Figure S1b).[11] This β-phase is characterized by a red-shifted luminescence spectrum[7] and an increased exciton diffusion length and results in devices with improved performance.[3,5,12,13] Therefore, PFO has high commercial potential in addition to research value to understand CP polymorphism.[14,15] As a result, significant efforts have been devoted to understanding and controlling the chemical and solution-processing parameters that induce chain planarization and promote β-phase content in PFO polymers.[16–18] The first observations of β-phase described it as a result of polymer crystallization, and thus, an intrinsically aggregation-driven phenomenon.[19–22] However, studies in dilute solutions have shown that a certain degree of β-phase can also be obtained from single chains in poor solvents at low temperatures.[23] It was found that β-phase arises following a two-step process that is initiated by the formation of intra-chain planar conformations that subsequently trigger an intermolecular aggregation process.[23,24] The use of single-molecule spectroscopy (SMS), with its unique ability to investigate polymer chains one by one[25–27], has been particularly useful for the study of PFO because its intrinsic phase heterogeneity cannot be resolved by conventional ensemble-averaging spectroscopy.[25,28–30] Single-molecule spectroscopy studies of poly(9,9-dioctyl)fluorene (PFO) molecules dispersed in a Zeonex matrix demonstrated the coexistence of α- and β-phase chains at 5 K.[31]

Considering the highly diluted nature of the samples used in these studies, it was concluded that β-phase formation does not need inter-chain interactions and that stress-induced backbone planarization could result from interactions with the host-matrix. Similar SMS studies using matrix-embedded PFO oligomers have shown that β-phase formation is a molecular length dependent process and

that nine or more repeat units are necessary to form a stable planarized structure, at least when prepared through the vapor swelling procedure.[28] Low-temperature photoluminescence (PL) excitation spectroscopy has also revealed that the entire polymer chain can behave as a single chromophore and that in-plane bending within the chromophore is

possible without altering the conjugation of the π-electron system.[32–34]

However, to date, the application of SMS in the context of PFO has been limited to embedding the polymeric material in a host matrix at very high dilution and mostly at low temperatures. Thus, the crucial question of PFO polymorphism in solution remains unsolved and how to answer it constitutes a challenging task. Understanding the correlation between single chain conformation and PL output is also particularly challenging in the case of PFO due to its 'hairy rod' properties and tendency to form supramolecular aggregates even at very low concentrations.[23] Here, we present the first spectroscopic characterization of individual PFO chains in good and poor solvents at room temperature. By combining single-end chemical functionalization of PFO chains with glass-reactive triethoxysilane groups and surface-passivation methods tailored to avoid non-specific adsorption of conjugated polymers, we have extracted the spectral features of each chain as a function of solvent properties, determined the relative population of each PFO phase at a given condition, and induced phase transition on single chains using a real-time solvent-exchange approach.

RESULTS AND DISCUSSION

Polymer design and chemical synthesis. One of the main reasons for the lack of single-molecule studies for single chains in solution is the need to immobilize the polymer so that the spectroscopic behavior and photoluminescence intensity of individual molecules can be monitored for prolonged periods of time. Single-molecule characterization of conjugated polymers in solution requires a method for tethering one end of the polymer to the substrate. We recently introduced an immobilization method for poly(3-hexylthiophene) (P3HT) using triethoxysilane (TES) groups.[35] Here, we developed a synthetic route to incorporate TES functionalities at a single end of the PFO polymer.

The synthesis of the triethoxysilane-terminated PFO polymer (**TES-PFO**) started with the polymerization of 2-(7-bromo-9,9-dioctyl-9H-fluoren-2-yl)-5,5-dimethyl-1,3,2-dioxaborinane (characterization show in Figure S2-3) as a bi-functional monomer **M** (Scheme 1) following the Suzuki protocol and using tetraethylammonium hydroxide as a base (Scheme 1). The polymerization was followed by end-capping and the resulting polymer **P1** was purified by methanol and acetone extraction to remove low-molecular weight fractions. Further functionalization of carbinol end groups was achieved by reaction with triethoxy(3-isocyanatopropyl) silane to yield the polymer **TES-PFO**. The molecular weight of the latter was estimated by comparison of integrals for the signals of methylene groups attached to the oxygen (quartet at 3.87 ppm) and nitrogen (multiplet at 3.38 – 3.27 ppm) atoms of the urethane functionality, which do not overlap with the aliphatic/water region of the spectrum (Figure S4-5), or with the signals of methylene groups in the polymer octyl chains (broad signal at 2.50 – 1.70 ppm). This estimation gives the value of

19400 Da, which is consistent with Mn value of 17400 Da, estimated by GPC (Figure S6-7). Due to hydrolytic deboronation upon polymerization in the basic conditions, the ratio of end-capping with **Br-PhCOOH** was estimated to be 24% (see Supporting Information for details, Scheme S1 and Figure S8).

Minimizing non-specific adsorption of CPs using perfluorinated surface passivation and SM setup. To observe fluorescence from single PFO molecules in solution, we immobilized single polymer chains at very low-density through silane chemistry (Scheme 1 and Figure 1, see Supporting Information for specific details of immobilization protocol). With such sparse surface coverage, fluorescence light from individual molecules did not overlap and isolated bright spots corresponding to single molecules can be easily monitored (Figure 1b). The glass substrates containing dispersed PFO chains were then placed in a custom-built chamber that was later filled with a specific solvent for imaging (see the Supporting Information for details of setup and sample chamber).[35] In our single-molecule setup, the field-of-view (FOV) has dimensions of 50 x 50 μm. In a typical experiment, 200-300 spots, each corresponding to a single molecule can be observed in the FOV which has an area of 2500 μm^2, corresponding to a density of 8.3 μm^2 per molecule (Figure 1). To extract spectral information from single chains, we coupled a spectrograph to our setup (Figure 1b) using a switchable beam splitter that directed 90% of the light into the spectrograph. In our previous work, we demonstrated specific immobilization of P3HT polymers using silane chemistry with no need for passivating the glass surface.[35] However, the intrinsically weak non-specific adsorption of P3HT chains to bare glass substrates constitutes an exception. Most widely used conjugated polymers exhibit strong non-specific interactions with the glass surface that can alter their conformation and preclude the immobilization of single chains at one specific end.[36] To minimize such polymer-glass interactions, we developed a method to passivate glass surfaces by coating them with an inert molecule. 1H,1H,2H,2H-perfluorodecyltriethoxysilane (PFDTES) was chosen primarily because its low surface energy should result in excellent anti-adherent properties (Figure 1a). Perfluorinated compounds such as PFDTES are commonly used as anti-fouling agents[37] and in the preparation of superhydrophobic nanoparticles[38] but their application as passivation agents for single-molecule microscopy studies has not been reported.

PFDTES-treated and untreated glass was exposed to a 50 pM PFO solution in toluene and incubated for 5 minutes. The number of fluorescence spots in both surfaces was counted using our single-molecule wide-field microscope setup. In untreated surfaces we observed average values of 420 spots per FOV (Figure 1c). The number of spots did not change significantly after successive steps of washing the chamber with a good solvent such as toluene, thus confirming a strong non-specific interaction between PFO and the glass surface. In contrast, for PFDTES-treated surfaces, the number of PFO molecules non-specifically adsorbed decrease by ~ 40-fold (Figure 1c), thus suggesting efficient passivation of the glass surface by PFDTES. Next, we evaluated whether this passivation method works for conjugated polymers in general or it is indeed specific to PFO, so we carried out an identical experiment replacing PFO with MEH-PPV, a conjugated polymer known to interact with

untreated glass substrates.[39] In untreated surfaces, we observed an average of 400 spots (Figure 1a and 1c). This value decreased to ~8 spots when passivating the glass surface (Figure 1c), suggesting that PFDTES-coating might be a promising and general method to avoid non-specific adsorption of conjugated polymers. Once confirmed that PFDTES prevents PFO from interacting with glass surfaces, we carried out an experiment in which 10 nM triethoxysilane-derivatized PFO (TES-PFO) was reacted with the glass surface in the presence of 10 mM PFDTES. Even when using a 200-fold higher concentration of TES-PFO (10 nM) compared to PFO in untreated surfaces (50 pM), the single-molecule image showed spatially separated chains of TES-PFO with a density of ~300 molecules per FOV. Importantly, coating the glass surface with PPDTES did not increase the background signal, something of critical importance when carrying out single-molecule experiments. The number of immobilized spots changed linearly with the concentration of TES-PFO (Figure S9). Similarly, a Poisson analysis of 300 molecules in 512x512 pixels suggested a probability value of 0.175 for having only one pixel of the entire FOV occupied by 2 molecules, thus confirming that each spot corresponds to a single immobilized TES-PFO chain. The combination of TES-immobilization with PFDTES-based passivation opens new possibilities regarding polymer observation at single-chain level in solution, since it exposes the chain to the solvent while efficiently minimizing interactions with the surface.

Single-molecule spectroscopy of PFO chains in organic solvents. Using these passivation and immobilization protocols, we characterized the photoluminescence behavior of TES-PFO molecules at single-molecule level as a function of solvent quality. We chose toluene and isopropanol (IPA) as representative examples of good and poor solvents, respectively. The moderately good solubility of PFO in toluene has been recently reported and its photoluminescence properties have been extensively studied in bulk-averaging conditions.[40,41] In contrast, PFO is poorly soluble in alcohols and characterization in these solvents has focused on their role as co-solvent inducing β-phase formation.[41–43] In these studies, the observed correlation between alcohol content and β-phase was explained based on inter-chain aggregation[44], but to which degree single PFO chains can adopt a β-phase structure in poor solvents or solvent mixtures remains unknown. Our approach using single immobilized TES-PFO provides a unique solution to investigate this aspect that cannot be addressed by any other technique. Once single TES-PFO chains are immobilized on the glass substrate, they can be exposed to any environmental condition with no interference from aggregation phenomena, even to those solvents where the polymer is virtually insoluble.

We compared the photoluminescence (PL) intensity trajectory of single TES-PFO chains in toluene and IPA. As shown in Figure 2, the intensity traces were remarkably different between both solvents. In isopropanol, 75% of the PL trajectories exhibited a very fast blinking dynamics between dark and bright states (Figure 2a, left panel) and the remaining traces display multi-level intensity trajectories (Figure S10). In contrast, 66% of PL trajectories in toluene were characterized by a single-level stable emission until photobleaching occurred (Figure 2a, right panel) and the remaining 33% displayed multi-level blinking dy-

namics (Figure S11). We used Hidden Markov modelling (HMM) to obtain the idealized intensity trajectory for each immobilized TES-PFO (Figure S12a). From the idealized trajectory, we extracted the distribution of dwell-times in the bright (τ_{on}) and dark (τ_{off}) states (Figure S12b). We obtained values in IPA of 200 and 130 milliseconds for τ_{on} and τ_{off}, respectively. Because some of the blinking transients were too fast to be accurately determined using HMM, we also carried out an autocorrelation analysis of the intensity fluctuations (Figure S13). This analysis revealed the presence of two intensity-fluctuation regimes with timescales differing by almost an order of magnitude. The fast dynamics component (τ_{fast} ~ 20-30 ms) is reminiscent of that previously observed for single PFO chains in a Zeonex matrix at room temperature. [34] Such dynamics were explained based on chain planarization in the β-phase leading to the entire polymer behaving as a single chromophore. This assignment was further supported by photon-antibunching measurements showing a strong dip at zero delay time. The slow component of the autocorrelation function (τ_{slow} ~ 400-500 ms) matches the combined $\tau_{on}+\tau_{off}$ obtained from HMM analysis. At present, we hypothesize that this component might reflect fluctuations in polymer conformation or dark states that are stabilized by interactions with the solvent.

We recorded the PL spectra of immobilized chains in each solvent using the wide-field microscope coupled to a spectrograph (Figure 1b). In both solvents, the PL spectrum of individual TES-PFO chains showed similar temporal stability within the 10 seconds observation window but their spectral features, taken in the interval from 415 to 480 nm, were significantly different (Figure 2b and Figure S14). In these experiments, we have taken the position of the 0-0 band as the peak of the emission spectra. In IPA, most polymers show the 0-0 band peaking at around 437 nm and the 0-1 peak at approximately 465 nm (Figure 2b, left panel), which are characteristic features of a β-phase emission. In contrast, a significant amount of immobilized chains in toluene showed the 0-0 and 0-1 bands slightly shifted to the blue and peaking at around 415 nm and 442 nm, respectively (Figure 2b, right panel). The position of these bands agrees with those observed for PFO in toluene in bulk-averaging conditions which have been assigned as intrinsic features of the α-phase conformation. To quantify the relative population of TES-PFO chains with PL spectra resembling those of the α- and β-phase in each solvent, we built single-molecule histograms by classifying individual emission spots on the basis of the peak position of the 0-0 band (Figure 3). For IPA, the single-molecule peak histogram showed a 70 % of TES-PFO molecules displaying β-phase-like spectra (Figure 3a). This value decreased to 25 % in toluene (Figure 3b). A measurement of intensity and emission spectra from the same molecule has not been carried out, simply because there is not enough emission signal to simultaneously collect fast blinking dynamics and spectral data with sufficiently good signal-to-noise ratio. However, the agreement between the percentage of molecules showing fast dynamics (75%) and β-phase like spectra (70%) indirectly suggests a correlation between both features. It is crucial to realize that extracting the phase distribution of PFO polymers in solution is only possible by analyzing the spectral information on a chain-to-chain basis and this can only be achieved using the combination of

surface-immobilization and passivation protocols introduced earlier in this work.

Recent studies using mixtures of ethanol with toluene or chloroform reported an increase in β-phase content when increasing the concentration of ethanol until reaching a maximum of ~ 44 % at 40 % w/v ethanol.[41] Because no β-phase content over this value has been observed over a wide range of solvents reported in the literature, it has been suggested that it constitutes an intrinsic β-phase saturation limit. Mechanistically, it has been proposed that in semi-dilute conditions (<2mg/mL), β-phase saturation arises from a reduced solubility that alters the balance between the formation of mesoscopic aggregates inducing β-phase formation and their compaction into denser aggregates that compromise planarization.[41,43]

In this context, our observation that isolated TES-PFO chains in an extremely poor solvent such as IPA exhibit β-phase emission to a much higher extent (70 %) than in bulk measurements (44 %) suggests that the latter saturation is indeed driven by inter-chain interactions that might be present only at certain PFO concentrations and solvent mixtures.

Conformational reorganization of single PFO chains in response to solvent conditions. To date, the observation of a single PFO chain alternating its conformation between both phases has not been reported. This is mostly due to the inability of matrix-based single-molecule techniques to modify the environment after the chains have been trapped within the matrix. Recently, we demonstrated that immobilization of single P3HT chains using one-end functionalization of CPs with silane groups allows monitoring of their conformational evolution triggered by sudden changes in their solvation environment.[35] This was based exclusively on PL intensity changes. Here, for PFO, we take the solvent-switching method one step further by monitoring also the spectral response of the same TES-PFO chain when exchanging between IPA and toluene.

The single-molecule PL trajectories obtained during real-time solvent switching displayed the characteristic intensity profiles as recorded previously in each solvent individually (Figure 4 and Figures S15-16). When switching from IPA to toluene (Figure 4a), the PL trajectory changed from an intensity profile showing fast intensity fluctuations to a stable single intensity level in toluene, and vice versa during the toluene→IPA exchange (Figure 4b). As previously reported for single PFO chains immobilized in a Zeonex matrix, the average intensity of PL profiles displaying fast blinking in IPA is significantly higher than those emitting as a single-intensity level in toluene.[34] We did not observe a substantial lag phase between solvent exchange and detecting a shift in the pattern of the PL intensity trajectory, suggesting that PFO polymers in solution adjust to changes in solvent in a timescale comparable to the solvent injection time (~1 s). By synchronizing and overlaying the PL traces with respect to the switching time we also observed a remarkable homogeneity in the timescale for PFO adjustment to the new solvation conditions (Figure 4a and 4b, right panels).

To confirm that the observed changes in PL intensity trajectories indeed represent PFO chains adjusting their conformation in real time, we recorded the PL spectra for the same PFO chain before and after the solvent switching

event. As shown in Figure 4c for the case of the IPA→toluene transition, the spectra collected before and after solvent exchange confirm the switching from a PL spectrum showing the characteristic features of β-phase emission to those of α-phase emission. Thus, we are confident that we are observing transitions between the α- and β-phases induced in single PFO chains (Figure 4d). Our data provides an unambiguous proof that β-phase emission can be induced in single PFO chains simply by solvent replacement, and in the absence of inter-chain interactions or matrix-induced stress. At present our data do not allow us to estimate the extent of β-phase content in each immobilized polymer. Therefore, we cannot rule out the presence of α-phase segments from which energy transfer to the planarized structure could occur as schematically shown in Figure 4d. However, the concept of isolated PFO chains being able to adopt a planarized conformation in solution is consistent with recent theoretical calculations suggesting that van der Waals contacts between neighboring alkyl side chains and the fluorene backbone are sufficient to stabilize the β-conformer in single chains even in the gas phase.[45] Our spectral data do not only confirm that PFO molecules can be induced to form β-phase domains simply by changing the solvation conditions, but we also demonstrate, for the first time, that individual PFO chains can transit between both phases in a remarkably fast timescale (< 1s).

Solvent-driven phase reversibility in isolated PFO chains. The ability to induce the transformation between the α- and β-phases in real time prompted us to evaluate the reversibility of the process in solution at the single chain level. Some evidence of phase reversibility has been previously obtained from bulk-averaging measurements of diluted PFO samples in methylcyclohexane (MCH) using a temperature jump between 295 K and 270 K to alter the phase equilibrium.[23] However, the reversibility of PFO planarization in single polymers has never been demonstrated. In Figure 5, we show representative PL trajectories obtained by repetitively changing the solvent environment between IPA and toluene.

We carried out four switching cycles resulting in each individual chain being sequentially exposed to five solvation conditions starting with IPA (Figure 5a-d). We observed a remarkable photostability with many TES-PFO chains remaining emissive after each switching event or photobleaching only in the last cycle. This is the first time this could be observed because the extremely fast photobleaching rate of immobilized P3HT chains when switching in real time from dimethyl-sulfoxide (DMSO) to o-dichlorobenzene (o-DCB) render P3HT unsuitable for reversibility analysis at the single-chain level. The remarkable photostability of PFO chains in both phases was already proven at 5 K using Zeonex matrix immobilization[31] but no data for single chains in solution at room temperature has been reported.

Insights into the reversibility process can be extracted from the recorded PL trajectories. First, most chains responded to each switching event. Secondly, the resulting PL profile displayed alternating intensity patterns that followed the solvation conditions and were characteristic of IPA (fast fluctuations) and toluene (single-state emission) (Figure 5a-b). Some exceptions included some chains

having higher or comparable intensities in IPA and toluene (Figure 5c) or the lack of blinking dynamics during the IPA solvation window (Figure 5d). Taken together, these observations confirm that individual chains can reversibly interconvert multiple times from one phase to another simply by periodic solvent exchange. Interestingly, PL profiles displayed similar intensity values between two consecutive steps in toluene which was not so apparent in the case of IPA. To quantify this, we plotted the intensity for a given molecule in toluene (i.e., step 2 in Figure 5a) against the intensity of the same molecule in the next toluene step (i.e., step 4 in Figure 5a) for all recorded molecules. It can be seen that the 2D contour plot for IPA (Figure 5e) shows a higher dispersity (mean intensity value of 214 with standard deviation of 236) when compared to the one for toluene, which has a mean intensity value of 142 with standard deviation of 178 (Figure 5f). It is important to realize that molecular-length polydispersity does not play a role when comparing the same chain and it cannot explain relative changes from molecules in the same FOV between switching steps. We argue that the observed differences in heterogeneity levels between IPA and toluene reflect different levels of structural diversity in poor and good solvents. Although disordered, the α-phase, predominant in toluene, might constitute a structurally more homogeneous state, and therefore, it leads to a low PL heterogeneity. On the other hand, in a poor solvent, the extent of β-phase content can differ from molecule to molecule and even the same chain might not reach similar planarization levels during the α-β-phase transformation.

CONCLUSIONS

In summary, we have developed a synthetic approach to incorporate functional groups into PFO and introduced a potentially general and simple passivation strategy to minimize non-specific adsorption of CPs to glass surfaces. The combination of these techniques has allowed us to extract the photoluminescence and spectral features of single PFO chains in good and poor solvents with no interference from inter-chain aggregation or matrix-induced stress, and for the first time, we induced conformational changes in real time. Our results confirm that β-phase domains can be formed in single chains, presumably via alkyl side chain interdigitation into the fluorene backbone and that this structure constitutes the predominant conformation observed in a poor solvent such as IPA. Moreover, because PFO chains immobilized at one end can freely adjust their conformation in response to solvation conditions, we studied the transformation between α- and β-phases by exposing the polymer to successive IPA-toluene switching steps. Individual PFO chains followed with remarkable fidelity the periodic exchange of solvents and cyclically adopted PL intensity profiles characteristic of α- and β-phase conformations. We compared the variability of the PL intensity values between molecules and within the same molecule for different solvent-switching events. Our data suggest that PFO molecules in good solvents such as toluene adopt a disordered but structurally homogeneous conformation leading to highly homogeneous PL behavior. In contrast, the substantial scatter of PL intensity values between consecutive switching events into the same poor solvent indicates a high structural heterogeneity that might reflect variations in glassy and β-phase content at the single-chain level.

ACKNOWLEDGMENTS

We acknowledge funding from EPSRC (grant no. EP/N009886/1 and EP/N009886/2). F. T-C thanks the EPSRC (grant no. EP/L015110/1).

Author Contributions

Conceptualization, J.C.P, I.D.W.S and P. J. S; Investigation, A.B., F.T.C., A.K., P.J.S, I.D.W.S. and J.C.P.; Resources J.C.P, I.D.W.S and P. J. S.; Writing – Original Draft, A.B., F.T.C., A.K., P.J.S, I.D.W.S. and J.C.P; Writing – Review & Editing, A. B., I. D. W. S and J. C. P.

Declaration of interests

The authors declare no competing financial interest

EXPERIMENTAL PROCEDURES

Details of synthetic routes and purification methods; Nuclear Magnetic Resonance characterization of polymers; passivation protocols, photoluminescence trajectories in toluene and isopropanol; blinking dwell-time single-molecule histograms in isopropanol; representative trajectories of changes in PL signal induced by solvent switching and spectral temporal evolution of single PFO polymers in isopropanol and toluene are given in the supporting information section.

Research Data

Research data supporting this publication is available at https://doi.org/10.17630/f5836bdf-36a2-48e6-a538-4d03255431bd

ABBREVIATIONS

SMS, single-molecule spectroscopy; PFO, poly(9,9'-dioctlyfluorene); P3HT, poly(3-hexylthiophene); TES, triethoxysilane; IPA, isopropanol; FOV, field of view.

REFERENCES

1. Facchetti, A. (2011). π-Conjugated Polymers for Organic Electronics and Photovoltaic Cell Applications. Chemistry of Materials *23*, 733–758.

2. Moliton, A., and Hiorns, R.C. (2004). Review of electronic and optical properties of semiconductingπ-conjugated polymers: applications in optoelectronics. Polymer International *53*, 1397–1412.

3. Scherf, U., Neher, D., and Becker, K. eds. (2008). Polyfluorenes (Springer).

4. Prins, P., Grozema, F.C., Nehls, B.S., Farrell, T., Scherf, U., and Siebbeles, L.D.A. (2006). Enhanced charge-carrier mobility in β -phase polyfluorene. Physical Review B *74*, 113203-113206

5. Cadby, A.J., Lane, P.A., Mellor, H., Martin, S.J., Grell, M., Giebeler, C., Bradley, D.D.C., Wohlgenannt, M., An, C., and Vardeny, Z.V. (2000). Film morphology and photophysics of polyfluorene. Physical Review B *62*, 15604–15609.

6. Khan, A.L.T., Sreearunothai, P., Herz, L.M., Banach, M.J., and Köhler, A. (2004). Morphology-dependent energy transfer within polyfluorene thin films. Physical Review B *69*. 085201-085209

7. Cadby, A.J., Lane, P.A., Wohlgenannt, M., An, C., Vardeny, Z.V., and Bradley, D.D.C. (2000). Optical studies of photoexcitations of poly(9,9-dioctyl fluorene). Synthetic Metals *111–112*, 515–518.

8. Winokur, M.J., Slinker, J., and Huber, D.L. (2003). Structure, photophysics, and the order-disorder transition to the β phase in poly(9,9-(di- n , n -octyl)fluorene). Physical Review B *67*, 184106-184117

9. Peet, J., Brocker, E., Xu, Y., and Bazan, G.C. (2008). Controlledβ-Phase Formation in Poly(9,9-di-n-octylfluorene) by Processing with Alkyl Additives. Advanced Materials *20*, 1882–1885.

10. Caruso, M.E., and Anni, M. (2007). Real-time investigation of solvent swelling induced β -phase formation in poly(9,9-dioctylfluorene). Physical Review B *76*, 054207-054211

11. Grell, M., Bradley, D.D.C., Ungar, G., Hill, J., and Whitehead, K.S. (1999). Interplay of Physical Structure and Photophysics for a Liquid Crystalline Polyfluorene. Macromolecules *32*, 5810–5817.

12. Tamai, Y., Ohkita, H., Benten, H., and Ito, S. (2015). Exciton Diffusion in Conjugated Polymers: From Fundamental Understanding to Improvement in Photovoltaic Conversion Efficiency. The Journal of Physical Chemistry Letters *6*, 3417–3428.

13. Bai, Z., Liu, Y., Li, T., Li, X., Liu, B., Liu, B., and Lu, D. (2016). Quantitative Study on β-Phase Heredity Based on Poly(9,9-dioctylfluorene) from Solutions to Films and the Effect on Hole Mobility. The Journal of Physical Chemistry C *120*, 27820–27828.

14. Scherf, U., and List, E.J.W. (2002). Semiconducting Polyfluorenes—Towards Reliable Structure-Property Relationships. Advanced Materials *14*, 477–487.

15. Kulkarni, A.P., and Jenekhe, S.A. (2003). Blue Light-Emitting Diodes with Good Spectral Stability Based on Blends of Poly(9,9-dioctylfluorene): Interplay between Morphology, Photophysics, and Device Performance. Macromolecules *36*, 5285–5296.

16. Knaapila, M., and Monkman, A.P. (2013). Methods for Controlling Structure and Photophysical Properties in Polyfluorene Solutions and Gels. Advanced Materials *25*, 1090–1108.

17. Tapia, M.J., Monteserín, M., Burrows, H.D., Seixas de Melo, J.S., Pina, J., Castro, R.A.E., García, S., and Estelrich, J. (2011). β-Phase Formation of Poly(9,9-dioctylfluorene) Induced by Liposome Phospholipid Bilayers. The Journal of Physical Chemistry B *115*, 5794–5800.

18. Tapia, M.J., Monteserín, M., Burrows, H.D., Almeida, J.A.S., Pais, A.A.C.C., Pina, J., Seixas de Melo, J.S., Jarmelo, S., and Estelrich, J. (2015). From molecular modelling to photophysics of neutral oligo- and polyfluorenes incorporated into phospholipid bilayers. Soft Matter *11*, 303–317.

19. Grell, M., Bradley, D.D.C., Inbasekaran, M., and Woo, E.P. (1997). A glass-forming conjugated main-chain liquid crystal polymer for polarized electroluminescence applications. Advanced Materials *9*, 798–802.

20. Redecker, M., Bradley, D.D.C., Inbasekaran, M., and Woo, E.P. (1999). Mobility enhancement through homogeneous nematic alignment of a liquid-crystalline polyfluorene. Applied Physics Letters *74*, 1400–1402.

21. Bradley, D.D.C., Grell, M., Long, X., Mellor, H., Grice, A.W., Inbasekaran, M., and Woo, E.P. (1997). Influence of aggregation on the optical properties of a polyfluorene. Proc. SPIE 3145, Optical Probes of Conjugated Polymers, 254-259

22. Grell, M., Bradley, D.D.C., Long, X., Chamberlain, T., Inbasekaran, M., Woo, E.P., and Soliman, M. (1998). Chain geometry, solution aggregation and enhanced dichroism in the liquidcrystalline conjugated polymer poly(9,9-dioctylfluorene). Acta Polymerica *49*, 439–444.

23. Dias, F.B., Morgado, J., Maçanita, A.L., da Costa, F.P., Burrows, H.D., and Monkman, A.P. (2006). Kinetics and Thermodynamics of Poly(9,9-dioctylfluorene) *β* -Phase Formation in Dilute Solution. Macromolecules *39*, 5854–5864.

24. Huang, L., Li, T., Liu, B., Zhang, L., Bai, Z., Li, X., Huang, X., and Lu, D. (2015). A transformation process and mechanism between the α-conformation and β-conformation of conjugated polymer PFO in precursor solution. Soft Matter *11*, 2627–2638.

25. Lupton, J.M. (2010). Single-Molecule Spectroscopy for Plastic Electronics: Materials Analysis from the Bottom-Up. Advanced Materials *22*, 1689–1721.

26. Dalgarno, P.A., Traina, C.A., Penedo, J.C., Bazan, G.C., and Samuel, I.D.W. (2013). Solution-Based Single Molecule Imaging of Surface-Immobilized Conjugated Polymers. Journal of the American Chemical Society *135*, 7187–7193.

27. Steiner, F., Vogelsang, J., and Lupton, J.M. (2014). Singlet-Triplet Annihilation Limits Exciton Yield in Poly(3-Hexylthiophene). Physical Review Letters *112*, 137402-137407.

28. Da Como, E., Scheler, E., Strohriegl, P., Lupton, J.M., and Feldmann, J. (2009). Single molecule spectroscopy of oligofluorenes: how molecular length influences polymorphism. Applied Physics A *95*, 61–66.

29. Honmou, Y., Hirata, S., Komiyama, H., Hiyoshi, J., Kawauchi, S., Iyoda, T., and Vacha, M. (2014). Single-molecule electroluminescence and photoluminescence of polyfluorene unveils the photophysics behind the green emission band. Nature Communications *5*, 4666-4672.

30. Becker, K., Lupton, J.M., Feldmann, J., Nehls, B.S., Galbrecht, F., Gao, D.Q., and Scherf, U. (2006). On-Chain Fluorenone Defect Emission from Single Polyfluorene Molecules in the Absence of Intermolecular Interactions. Advanced Functional Materials *16*, 364–370.

31. Becker, K., and Lupton, J.M. (2005). Dual Species Emission from Single Polyfluorene Molecules: Signatures of Stress-Induced Planarization of Single Polymer Chains. Journal of the American Chemical Society *127*, 7306–7307.

32. Da Como, E., Borys, N.J., Strohriegl, P., Walter, M.J., and Lupton, J.M. (2011). Formation of a Defect-Free π-Electron System in Single β-Phase Polyfluorene Chains. Journal of the American Chemical Society *133*, 3690–3692.

33. Da Como, E., Becker, K., Feldmann, J., and Lupton, J.M. (2007). How Strain Controls Electronic Linewidth in Single β-Phase Polyfluorene Nanowires. Nano Letters *7*, 2993–2998.

34. Adachi, T., Vogelsang, J., and Lupton, J.M. (2014). Chromophore Bending Controls Fluorescence Lifetime in Single Conjugated Polymer Chains. The Journal of Physical Chemistry Letters *5*, 2165–2170.

35. Tenopala-Carmona, F., Fronk, S., Bazan, G.C., Samuel, I.D.W., and Penedo, J.C. (2018). Real-time observation of conformational switching in single conjugated polymer chains. Science Advances *4*, 5786-5798.

36. Araújo, F.L., Valente, G.T., Faria, R.M., and Guimarães, F.E.G. (2015). How surface interactions freeze polymer molecules at room temperature: a single molecule approach. IOP Conference Series: Materials Science and Engineering *97*, 012003.

37. Yong, J., Chen, F., Yang, Q., Huo, J., and Hou, X. (2017). Superoleophobic surfaces. Chemical Society Reviews *46*, 4168–4217.

38. Brassard, J.-D., Sarkar, D.K., and Perron, J. (2012). Fluorine Based Superhydrophobic Coatings. Applied Sciences *2*, 453–464.

39. Onda, S., Kobayashi, H., Hatano, T., Furumaki, S., Habuchi, S., and Vacha, M. (2011). Complete Suppression of Blinking and Reduced Photobleaching in Single MEH-PPV Chains in Solution. The Journal of Physical Chemistry Letters *2*, 2827–2831.

40. Knaapila, M., Dias, F.B., Garamus, V.M., Almásy, L., Torkkeli, M., Leppänen, K., Galbrecht, F., Preis, E., Burrows, H.D., Scherf, U., *et al.* (2007). Influence of Side Chain Length on the Self-Assembly of Hairy-Rod Poly(9,9-dialkylfluorene)s in the Poor Solvent Methylcyclohexane. Macromolecules *40*, 9398–9405.

41. Li, X., Bai, Z., Liu, B., Li, T., and Lu, D. (2017). From Starting Formation to the Saturation Content of the β-Phase in Poly(9,9-dioctylfluorene) Toluene Solutions. The Journal of Physical Chemistry C *121*, 14443–14450.

42. Liu, B., Li, T., Zhang, H., Ma, T., Ren, J., Liu, B., Liu, B., Lin, J., Yu, M., Xie, L., *et al.* (2018). Polyfluorene (PF) Single-Chain Conformation, β Conformation, and Its Stability and Chain Aggregation by Side-Chain Length Change in the Solution Dynamic Process. The Journal of Physical Chemistry C *122*, 14814–14826.

43. Li, T., Huang, L., Bai, Z., Li, X., Liu, B., and Lu, D. (2016). Study on the forming condition and mechanism of the β conformation in poly (9,9-dioctylfluorene) solution. Polymer *88*, 71–78.

44. Huang, L., Huang, X., Sun, G., Gu, C., Lu, D., and Ma, Y. (2012). Study of β phase and Chains Aggregation Degrees in Poly(9,9-dioctylfluorene) (PFO) Solution. The Journal of Physical Chemistry C *116*, 7993–7999.

45. Chunwaschirasiri, W., Tanto, B., Huber, D.L., and Winokur, M.J. (2005). Chain Conformations and Photoluminescence of Poly(di- n -octylfluorene). Physical Review Letters *94*, 107402- 107406.

Figure legends

Scheme 1. Synthesis of triethoxysilane terminated PFO chains (TES-PFO).

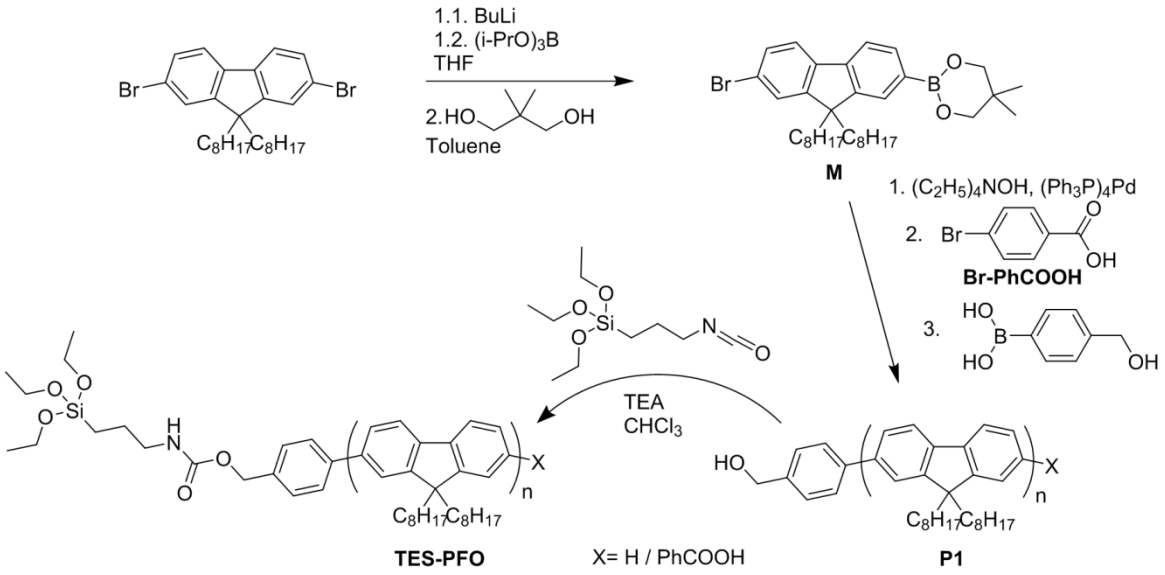

Figure 1. Surface-passivation of glass substrates by PFDTES minimizes non-specific adsorption of conjugated polymers. (a) Schematics of PFDTES passivation and representative single-molecule images obtained for non-specifically adsorbed PFO on bare glass (left) and PFDTES-treated glass (middle) compared to TES-immobilized PFO on a PFDTES-treated slide (right). (b) Photoluminescence intensity and spectral characterization of surface-immobilized single PFO chains in solution. Schematics of the wide-field microscope equipped with a tight-seal sample chamber and a 10:90 beam splitter for PL and spectra collection. Representative photoluminescence trajectory and spectra obtained from immobilized molecules are shown. (c) Average number of single-molecule spots representing the amount of adsorbed polymers obtained in those conditions described in (a).

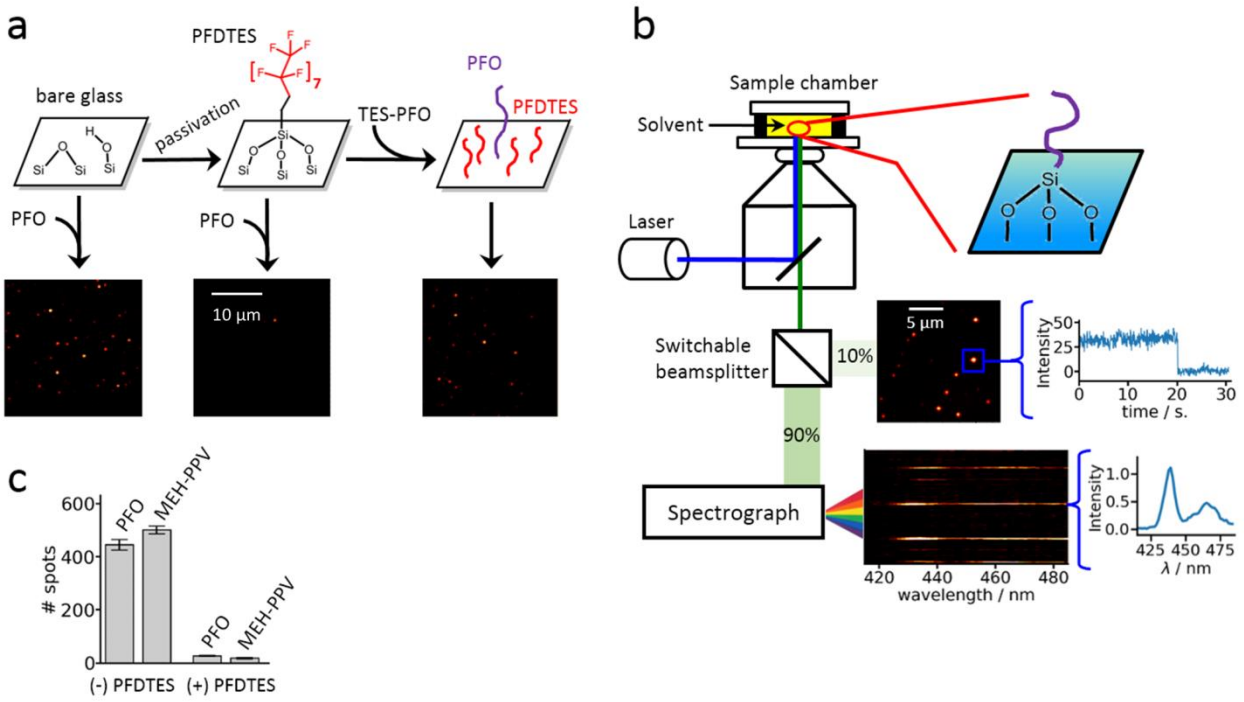

Figure 2. Single-molecule photoluminescence characterization of glass-immobilized TES-PFO chains in solution. (a) Representative TES-PFO photoluminescence trajectories in isopropanol (left) and toluene (right). (b) Temporal evolution of the PL spectra of a single TES-PFO molecule using 1 second time integration and corresponding integrated spectra over the 10 s time window in IPA (left) and toluene (right). The single-molecule spectra in IPA shows a peak at 437 nm and in toluene at 415 nm, which are characteristic of β-phase and α-phase, respectively.

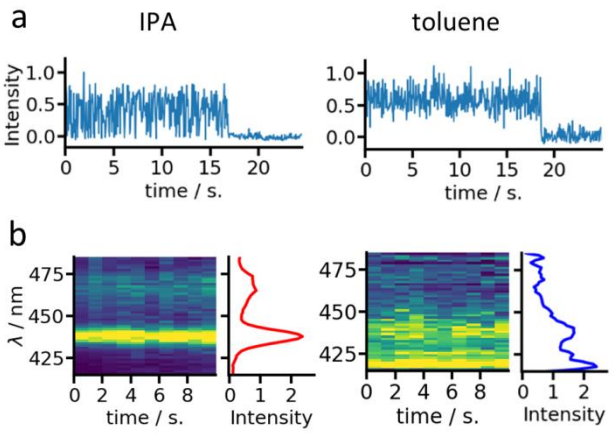

Figure 3. Single-molecule peak histograms showing the relative population of TES-PFO molecules showing spectral features characteristic of the α-phase and the β-phase in IPA (a) and toluene (b). Single-molecule histograms were constructed from 325 molecules in IPA and 220 in toluene.

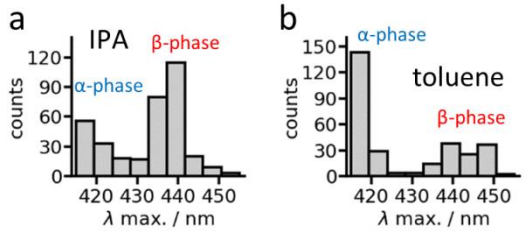

Figure 4. Real-time conformational reorganization of single PFO chains as a function of solvent conditions. (a) Left panel: Representative PL trajectory of a single PFO immobilized chain initially imaged in IPA and switched to a toluene environment at time 7 seconds. Right panel: Heat map plot resulting from the overlay of hundreds of PFO chains synchronized at the injection time. (b) Left panel: Representative PL trajectory of a single PFO immobilized chain initially imaged in toluene and switched to an IPA environment at time 5.5 seconds. Right panel: Heat map plot resulting from the overlay of 200 PFO chains synchronized at the injection time. (c) Spectra of a single PFO chain monitored in IPA (orange) and after solvent exchange with toluene (blue) showing the spectral features characteristic of β-phase and α-phase, respectively. (d) Schematics of the solvent-induced real-time switching experiment and the associated changes in PFO conformation.

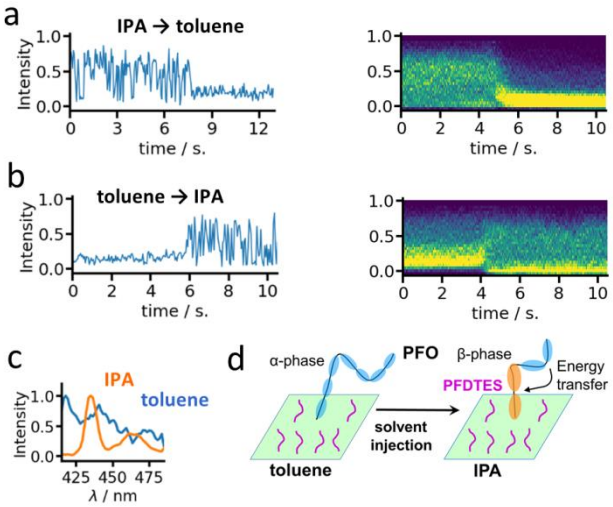

Figure 5. Reversible interconversion between α-phase and β-phase in single PFO chains induced by successive steps of solvent exchange. (a, d) Representative PL trajectories obtained by sequential switching between IPA (orange) and toluene (green). The asterisk in (b) and (d) indicates a photobleaching step. (e, f) Contour plots of the average PL intensity of the same PFO chain between two consecutive steps in IPA (e) and toluene (f) generated from 300 and 320 molecules, respectively. The single-molecule PL intensity histograms are also shown for both solvents.